Two-color resonant four-wave mixing spectroscopy of highly predissociated levels in the A A 1 2 state of C H 3 S

Ching-Ping Liu, Scott A. Reid, and Yuan-Pern Lee

Citation: The Journal of Chemical Physics **122**, 124313 (2005); doi: 10.1063/1.1867333
View online: http://dx.doi.org/10.1063/1.1867333
View Table of Contents: http://scitation.aip.org/content/aip/journal/jcp/122/12?ver=pdfcov
Published by the AIP Publishing

Two-color resonant four-wave mixing spectroscopy of highly predissociated levels in the $\tilde{A}\,^2A_1$ state of CH_3S

Ching-Ping Liu
Department of Chemistry, National Tsing Hua University, Hsinchu 30013, Taiwan

Scott A. Reid
Department of Chemistry, Marquette University, Milwaukee, Wisconsin 53201

Yuan-Pern Lee[a)]
Department of Applied Chemistry, National Chiao Tung University, Hsinchu 30010, Taiwan and Institute of Atomic and Molecular Sciences, Academia Sinica, Taipei 106, Taiwan

(Received 10 November 2004; accepted 13 January 2005; published online 30 March 2005)

We report results of two-color resonant four-wave mixing experiments on highly predissociated levels of the methylthio (or thiomethoxy) radical CH_3S in its first excited electronic state $\tilde{A}\,^2A_1$. Following photolysis of jet-cooled dimethyl disulfide at 248 nm, the spectra were measured with a hole-burning scheme in which the probe laser excited specific rotational transitions in band 3^3. The spectral simplification afforded by the two-color method allows accurate determination of line positions and homogeneous linewidths, which are reported for the C–S stretching states 3^v($v=3-7$) and combination states 1^13^v($v=0-2$), 2^13^v($v=3-6$), and $1^12^13^v$($v=0,1$) involving the symmetric CH_3 stretching (ν_1) mode and the CH_3 umbrella (ν_2) mode. The spectra show pronounced mode specificity, as the homogeneous linewidth of levels with similar energies varies up to two orders of magnitude; ν_3 is clearly a promoting mode for dissociation. Derived vibrational wave numbers ω_1', ω_2', and ω_3' of the $\tilde{A}$ state agree satisfactorily with *ab initio* predictions. © *2005 American Institute of Physics*. [DOI: 10.1063/1.1867333]

I. INTRODUCTION

Oxidation of naturally occurring organic sulfur compounds[1,2] such as dimethyl sulfide (CH_3SCH_3), dimethyl disulfide (CH_3SSCH_3), and methanethiol (CH_3SH) in the atmosphere produces the methylthio (or thiomethoxy) radical, CH_3S, as a reactive intermediate.[3,4] As this species is a key intermediate in reactions relevant to modeling the atmospheric sulfur cycle,[5] unambiguous analysis of its spectra and information concerning photochemical processes of its excited states are valuable both for the monitoring of the radical in reactions of environmental importance and for understanding its chemistry.

From a basic perspective, CH_3S is a prototype for investigation of mode selectivity in predissociation because its first electronically excited state, $\tilde{A}\,^2A_1$, is crossed by quartet and doublet repulsive states correlating with the $CH_3(\tilde{X}\,^2A_2'')+S(^3P)$ asymptote. This situation is analogous to that found for the methoxy radical (CH_3O) and other members of this family.[6,7] Like methoxy, CH_3S has an ^2E ground electronic state and is thus subject to a Jahn–Teller distortion. Theoretical interest in this molecule has been motivated in part by the interactions between Jahn–Teller and spin-orbit effects in the degenerate $\tilde{X}\,^2E$ ground state.[8] Several *ab initio* calculations have produced estimates of energies, geometries, and vibrational wave numbers of the $\tilde{X}\,^2E$ and/or $\tilde{A}\,^2A_1$ states of CH_3S.[9–14]

There have been many experiments to record spectra of the methylthio radical including electronic absorption[15,16] and emission,[17] photoelectron and photodetachment,[18–20] microwave,[21] laser-induced fluorescence (LIF),[22–26] photofragment yield,[27] fluorescence depletion,[28] and degenerate four-wave mixing.[29] These experiments have provided information on geometries, spin-orbit splitting, and some spectral parameters for CH_3S in both $\tilde{X}\,^2E$ and $\tilde{A}\,^2A_1$ states. Vibronic analysis of LIF spectra of the $\tilde{A}$-$\tilde{X}$ system performed in this laboratory identified all six vibrational modes of the $\tilde{X}\,^2E$ state, but only ν_2 (CH_3 umbrella)$=1098$ cm^{-1} and ν_3 (C–S stretch)$=401$ cm^{-1} were characterized for the $\tilde{A}\,^2A_1$ state.[26] An abrupt decrease of intensity in the fluorescence excitation spectrum was observed above 27 321 cm^{-1}, and attributed to predissociation of the $\tilde{A}\,^2A_1$ state. No emission was observed above 28 016 cm^{-1} (1490 cm^{-1} above the $\tilde{A}\leftarrow\tilde{X}$ origin).

Pushkarsky *et al.*[28] employed fluorescence depletion to extend observed features of $\tilde{A}\,^2A_1$ to 2979 cm^{-1} above the transition origin; the two features of greatest wave numbers, 3^7 and 2^13^5, have lifetimes ~0.5 ps. Bise *et al.*[27] recorded photofragment yield spectra of CH_3S produced on laser photodetachment of a rapid beam of mass-selected CH_3S^-, and observed extended vibronic bands of the $A\leftarrow X$ system up to 31 763 cm^{-1} (5237 cm^{-1} above the origin) which were as-

a)Author to whom correspondence should be addressed; Electronic mail: yplee@mail.nctu.edu.tw

signed to vibrational progressions of 3^v and $2^1 3^v$ ($0 \leqslant v \leqslant 15$). We employed degenerate four-wave mixing to investigate highly predissociative levels of CH_3S in the $\tilde{A}\,^2A_1$ state[29] and observed bands from 1180 to 5020 cm^{-1} above the origin; the results showed that the vibrational structure at higher energies was inconsistent with a continuation of the 3^v and $2^1 3^v$ progressions, and we tentatively identified new progressions $1^1 3^v$, $4^1 3^v$, and $2^1 3^v 4^1$ involving symmetric CH_3 stretching (ν_1) and asymmetric CH_3 stretching (ν_4) modes.

As the spectroscopy of CH_3S has progressed, so has research on its photochemistry. Measurements of radiative lifetime show a significant decrease for vibrational levels of the $\tilde{A}$ state $\geqslant$800 cm^{-1} above the origin.[23,24,26,30] Bise *et al.*[27] used an indirect method to measure the lifetimes of highly predissociative levels of the $\tilde{A}\,^2A_1$ state; their reported lifetimes are significantly longer than those reported by Pushkarsky *et al.*[28] who applied fluorescence depletion to measure lifetime broadening for the $3^v (v \leqslant 7)$ and $2^1 3^v (v \leqslant 5)$ progressions. The latter authors demonstrated that the predissociation was mode selective, with ν_3 a promoting mode,[28] and also proposed that, in the region in which excitation involves less than three quanta of ν_3, a second nonradiative decay channel for the $\tilde{A}\,^2A_1$ state, possibly leading to CH_2S+H, might exist. In our previous work of DFWM,[29] homogeneous broadening of rovibronic lines leading to overlapped band structures prevented detailed information on lifetimes of these predissociative states from being obtained.

Two-color resonant four-wave mixing (TC-RFWM) has been demonstrated to be an excellent tool to investigate highly predissociative states; its double-resonance nature has advantages over DFWM in selecting a specific rovibronic state, hence providing unambiguous spectral assignments and linewidth measurements. When used in a hole-burning scheme, in which the pump and probe beams share a common lower level and the signal is thus derived from the ground-state grating, the signal intensity is unaffected by the lifetime of the upper level.[31] We have applied TC-RFWM to detect highly predissociative electronic states $B\,^2\Sigma^+$, $C\,^2\Sigma^+$, and $D\,^2\Pi$ of CH radical in a flame;[32–35] the observed rovibronic transitions numbered two to three times those reported previously with laser-induced fluorescence or conventional absorption methods. We demonstrated also that, although its signal has a quadratic dependence on concentration of species of interest, TC-RFWM can be applied to both stable[36,37] and unstable[38] species in supersonic jets. In this work we applied TC-RFWM in the hole-burning scheme to investigate highly predissociative levels of CH_3S in a supersonic jet. In addition to confirming our assignment of progressions involving the symmetric CH_3 stretching (ν_1) mode, lifetimes of these states are measured for the first time, confirming the mode-selective nature of the predissociation.

II. EXPERIMENTS

We employed TC-RFWM with a ground-state grating (or hole-burning) scheme in which the pump (grating forming) and probe transitions shared a common lower level. For the probe transition, we selected specific rotational lines in the 3^3 band of the $\tilde{A} \leftarrow \tilde{X}$ transition. Although this band is predissociative, as evidenced by a minute fluorescence quantum yield,[26] it shows resolved rotational structure in DFWM spectra.[29] Moreover, the intense 3^3 band allows the use of a weaker probe beam; scattered light due to the probe beam is hence diminished. For all recorded TC-RFWM spectra, we set the probe wavelength to achieve resonance with a selected rotational transition in the 3^3 band and scanned the wavelength of the grating laser.

Details of the TC-RFWM experiment have been reported previously.[32,33] The pump beams were generated with a dye laser (Lambda Physik, Scanmate 2E, tunable in a spectral region 338–361 nm) pumped with a XeCl excimer laser at 308 nm (Lambda Physik, LPX 105). The frequency-doubled output of a dye laser (Lambda Physik, Scanmate 2E-OG, ~361 nm) pumped with the second harmonic (532 nm) of a Nd:YAG (YAG—yttrium aluminum garnet) laser (Spectra Physics, GCR-5) was employed as a probe. The dye lasers have temporal pulse widths 6–7 ns and fundamental spectral linewidths ~0.1 cm^{-1}. In some critical experiments when small jitter between pump and probe beams was required, the 532 nm output of the Nd:YAG laser was split into two beams with an energy ratio $\approx 2:1$ to pump two dye lasers (Spectra Physics PDL-3, and Scanmate 2E-OG); their outputs were frequency-doubled with separate BBO crystals to provide required wavelengths for grating and probe beams. The laser wavelengths were calibrated with a wavemeter (Burleigh WA-5500; accuracy ±0.2 cm^{-1}).

These experiments utilized a forward-box geometry, in which a beam splitter and a few total reflectors were employed to obtain two nearly parallel grating beams (ω_1 and ω_2) that cross at a small angle (~1°) near the nozzle of a supersonic jet. A temporally coincident probe beam (ω_3) propagating in the same direction crossed the grating beams at an angle satisfying the phase-matching condition. The three input beams should overlap spatially and temporally in the medium of interest. The resultant signal beam (ω_4) was allowed to travel 2–3 m before being spatially filtered with an iris, convex lens (f=10 cm) and a pinhole (diameter 0.15 mm) in combination, and was subsequently filtered with a suitable bandpass interference filter [passband ~365 nm, full width at half maximum (FWHM) 10 nm] or a monochromator (Jobin–Yvon, HR 320, 0.32 m focal length, 600 grooves mm^{-1}) before detection with a photomultiplier tube (Hamamatsu, R955P). The photomultiplier signal was amplified and averaged with a gated boxcar averager (Stanford Research Systems, SR250) and the data were subsequently transferred to a computer for further processing. The relative timing among the lasers, pulsed nozzle, and data acquisition systems was controlled with a digital delay generator (Stanford Research Systems, DG535). To diminish scattered laser light, we employed a crossed polarization scheme (YXXY), using Fresnel rhombs to rotate the polarization and Glan-laser polarizers to select the polarization of each beam. The polarization notation used here employs the conventional labeling scheme $(\omega_4, \omega_1, \omega_3, \omega_2)$.[39]

A mixture of dimethyl disulfide (DMDS) in helium was generated by bubbling helium through a liquid DMDS sample at ~296 K. Additional helium was added down-

stream to dilute further the mixture before expansion through a pulsed nozzle (General Valve, orifice diameter 1 mm). The concentration of DMDS was estimated to be less than 1%. The opening duration of the pulse valve was 500 μs and the stagnation pressure was typically 2 atm, which led to a typical background pressure $\sim 1\times 10^{-4}$ Torr. CH_3S radicals were produced on photolysis of DMDS at 248 nm using a KrF excimer laser (Lambda Physik, LPX 150T). The photolysis laser beam ~ 8 mJ pulse^{-1} was loosely focused with a cylindrical lens to a point several nozzle diameters downstream from the orifice. From its laser-induced fluorescence spectrum, the temperature of CH_3S was estimated to be 10–15 K, depending on experimental conditions. DMDS (Aldrich, 99%) and He (Scientific Gas Products, 99.9995%) were used without further purification.

III. RESULTS AND DISCUSSION

We reported previously DFWM spectra of jet-cooled CH_3S in its $\tilde{A}\,^2A_1$ state.[29] The first prominent feature observed in the DFWM spectrum was the 3^3 band, of which Fig. 1(a) displays a high-resolution scan showing the rotational structure. TC-RFWM scans were performed on tuning the wavelength of the grating beams with the probe beam tuned to excite rotational lines at 27 707.2 and 27 703.8 cm^{-1}, in the 3^3 band observed in DFWM [marked *a* and *b*, respectively, in Fig. 1(a)]. These two lines correspond mainly to transitions $K_a'=0\leftarrow K_a''=1$ from $J''=9/2$ and 3/2 (parity +) and $J''=9/2$ (parity −), respectively, according to spectral simulation with SpecView.[40] Figure 1(b) illustrates TC-RFWM spectra recorded by scanning the wavelength of grating beams over the 3^4 and 3^5 bands; one dominant transition and some additional weaker features were observed. Observed rovibronic lines for all vibrational bands measured in this work were thus assumed to correspond to rotational transitions identical to the selected probe transition; specifically, when a line corresponding to $v_3'=3$ and $K_a'=0$ is probed, observed TC-RFWM lines correspond to upper levels with $v_3'\geqslant 3$ and $K_a'=0$. For extremely predissociated lines, acceptable ratios of signal to noise were achieved only when line *b* was probed; hence we report vibrational wave numbers of all vibrational levels of the $\tilde{A}\,^2A_1$ state based on experiments with line *b* probed. Because several states were marked by the grating beams, occasionally additional weak lines were observed (e.g., the 3^5 line in Fig. 1 and the 2^13^3 line in Fig. 2). According to spectrum simulation, they are likely due to transitions from $J''=7/2$, $K_a''=2$ and $J''=5/2$, $K_a''=2$ for lines at low-energy and high-energy sides, respectively.

A portion of the TC-RFWM spectra of CH_3S is illustrated in Fig. 2 for the combination bands 2^13^v ($v=3$–5) and 1^13^v ($v=0$–2). The state-selected TC-RFWM spectra are much simpler than those from LIF or DFWM, allowing more accurate determination of line positions and homogeneous line widths. These spectra clearly demonstrate a pronounced increase in line width with increasing quanta of v_3, consistent with previous reports.[27,28] In the following discussion, we focus first on the vibrational assignments and second on the lifetimes determined from measured linewidths. The fitting procedure used to extract wave numbers and homogeneous widths of lines is discussed in Sec. III C.

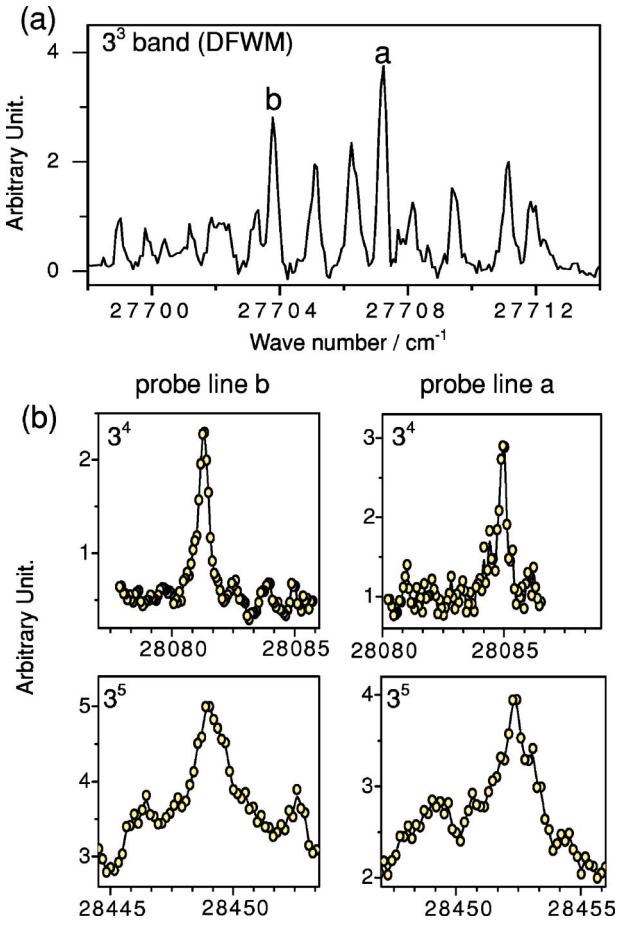

FIG. 1. (a) DFWM spectrum of the 3^3 band of the $\tilde{A}\leftarrow\tilde{X}$ transition of jet-cooled CH_3S. Labels "*a*" corresponds mainly $|J',\text{parity},K_a',\Sigma\rangle - |J'',\text{parity},K_a'',\Sigma'\rangle = |9/2,-,0,1/2\rangle - |9/2,+,1,1/2\rangle$, $|1/2,-,0,1/2\rangle - |3/2,+,1,1/2\rangle$, $|3/2,-,0,-1/2\rangle - |3/2,+,1,1/2\rangle$, and $|11/2,-,0,-1/2\rangle - |9/2,+,1,1/2\rangle$ and "*b*" corresponds to $|9/2,+,0,-1/2\rangle - |9/2,-,1,1/2\rangle$, $|7/2,+,0,1/2\rangle - |9/2,-,1,1/2\rangle$, $|3/2,+,1,-1/2\rangle - |5/2,-,2,1/2\rangle$, and $|3/2,-,1,-1/2\rangle - |5/2,+,2,1/2\rangle$. (b) TC-RFWM spectra recorded with a YXXY polarization scheme; lines *a* and *b* in (a) were selected separately as the probe transition while scanning the wavelength of the grating beams.

A. Progressions 3^v and 2^13^v

Two intense progressions, assigned as 3^v and 2^13^v, have been characterized previously by LIF,[26] photofragment yield spectra,[27] fluorescence depletion spectra (FDS),[28] and our recent work with DFWM.[29] Wave numbers reported previously for the progression 3^v are nearly identical to those determined using TC-RFWM for $v=4$–7 and within 4 cm^{-1} for 3^6 and 3^7 bands. The slight discrepancy for line positions between our TC-RFWM and DFWM experiments reflects the fact that in our DFWM work we could only estimate line positions from the contour of highly predissociative bands showing no rotational structure. For both measurements uncertainty in determining peak positions is greater for higher vibrational levels because of the severe lifetime broadening. Vibrational wave numbers, derived by subtracting 26 523.2 cm^{-1} (the corresponding line *b* in the origin band of LIF) from an observed wave number of each line, and their

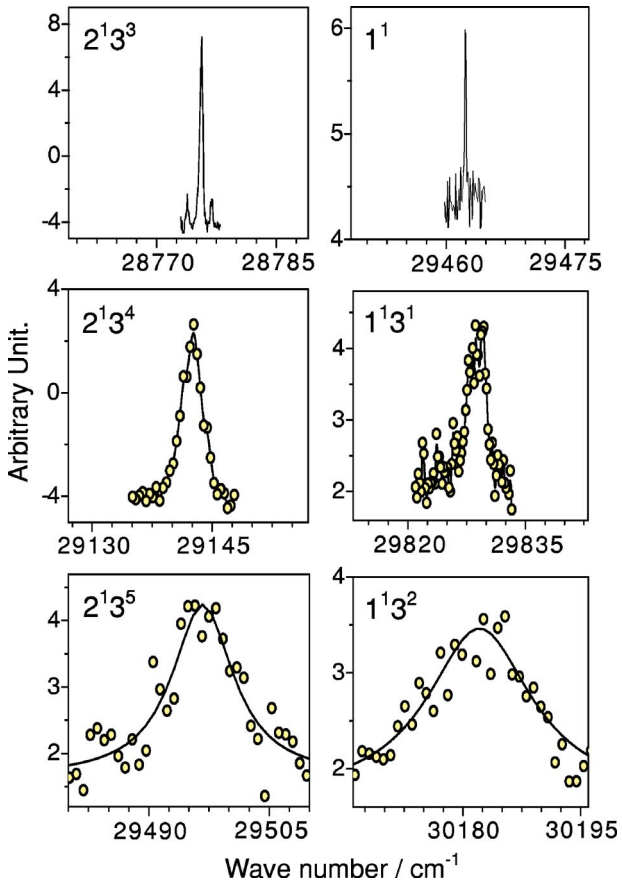

FIG. 2. Representative TC-RFWM spectra of the $\tilde{A} \leftarrow \tilde{X}$ system of jet-cooled CH_3S recorded with a YXXY polarization scheme. The probe beam was fixed at 27 703.8 cm^{-1} (line *b* in Fig. 1) and the scan steps are 0.001 nm for narrow bands and 0.01 nm for broad bands. Spectra in the left and right panels show $2^1 3^v$ and $1^1 3^v$ progressions, respectively.

corresponding uncertainties in measurements are listed in Table I. The observed uncertainty in peak position was determined from the fit (see below); for narrow lines the error was taken as the uncertainty of wave number measurements, 0.2 cm^{-1}. The origin of this transition (ν_{00}) lies at 26 526.7 cm^{-1},[29] corresponding to the a line (transition $K'_a = 0 \leftarrow K''_a = 1$, parity $+$) in the 0^0 band.

We combined the results of LIF, DFWM, and TC-RFWM to fit the 3^v progression by least squares to an equation,

$$\nu = \nu_{00} + (\omega'_{3(0)} - x'_{33})v'_3 - x'_{33}(v'_3)^2, \tag{1}$$

in which v'_3 is the vibrational quantum number of the C–S stretching (ν_3) mode and $\omega'_{3(0)}$ indicates the harmonic vibrational wave number when only ν_3 is considered. Fitted spectral parameters are listed in Table I. Unless otherwise noted, all listed uncertainties represent one standard deviation in fitting. We found that observed high-energy levels ($v=7$ and 8) deviate from Eq. (1) beyond uncertainties in wave number measurements; these lines were therefore excluded in the fitting. Deviations of experimental from calculated values are less than 0.7 cm^{-1} for $v \leqslant 6$. Wave numbers predicted for 3^7 and 3^8 according to Eq. (1) with derived spectral parameters are listed in brackets in Table I for comparison.

The $2^1 3^v$ progression in the TC-RFWM spectrum begins at $v=3$ and extends to $v=6$. Our previous DFWM experiments[29] showed $2^1 3^v$ bands up to $v=7$, with wave numbers that deviate within 3 cm^{-1} for $2^1 3^5$ and $2^1 3^6$ bands from this work. The discrepancy is more significant for unresolved DFWM bands associated with the higher vibrational levels, as also found for the 3^v progression discussed above. Vibrational energies of upper states in the $3^v (v \leqslant 6)$ and $2^1 3^v (v \leqslant 4)$ progressions are described with an equation (with $i=2$, $x'_{22}=0$, and $v'_2=1$ in this case):

$$\Delta\nu = A + \omega'_3(v'_3 + 0.5) - x'_{33}(v'_3 + 0.5)^2 + \omega'_i(v'_i + 0.5) - x'_{ii}(v'_i + 0.5)^2 - x'_{i3}(v'_i + 0.5)(v'_3 + 0.5), \tag{2}$$

in which $\Delta\nu$ is a vibrational wave number relative to the origin, A is a constant to account for zero-point energy, and $\omega'_3 = \omega'_{3(0)} + 0.5x'_{i3}$. We exclude x'_{22} from the fitting because there is no information on x'_{22} from this progression. Observed vibrational wave numbers and fitted spectral parameters are listed in Table I. Derived spectral parameters in progressions 3^v and $2^1 3^v$ are essentially the same as those from our previously reported DFWM work,[29] but deviations between observed and calculated wave numbers, less than 1 cm^{-1}, are diminished through accurate determination of band positions. Similar to the progression 3^v, lines corresponding to $2^1 3^v (v=5-7)$ were excluded from the fitting because of large deviations from Eq. (2); wave numbers predicted for these lines are listed in brackets in Table I for comparison. Predicted wave numbers of these lines in the $2^1 3^v$ progression are greater than observed values, whereas predicted values of lines 3^7 and 3^8 are smaller than observed values. A Fermi resonance between members of 3^{v+3} and $2^1 3^v$ ($v \geqslant 4$ or 5) might take place.

B. New progressions $1^1 3^v$ and $1^1 2^1 3^v$

In our DFWM experiments,[29] from observed spacings the intense lines denoted A' (29 492.2 cm^{-1}) and B' (29 826.6 cm^{-1}) appeared to belong to one progression, whereas lines C (30 180.3 cm^{-1}), D (30 492.9 cm^{-1}), and E (30 797.5 cm^{-1}) appeared to belong to another progression; they were tentatively assigned to $1^1 3^v$ and $4^1 3^v$, respectively. These bands (except band E) are compared in Fig. 3 with TC-RFWM spectra recorded in this work. Based on this assignment, three features 3^8 (29 514 cm^{-1}), $2^1 3^5$ (29 503 cm^{-1}), and 1^1 (29 492 cm^{-1}) might appear and overlap each other in the region near 29 500 cm^{-1}. We observed only two features in TC-RFWM spectra when line *b* was probed: one at 29 462.2 cm^{-1} has a laser-limited linewidth and the other at 29 500.4 cm^{-1} is significantly broader (Fig. 2). The broad feature is readily assigned to the $2^1 3^5$ band. The narrow line at 29 462.2 cm^{-1}, showing a vibrational wave number of 2939.0 cm^{-1}, corresponds to a weak shoulder in the DFWM spectrum. Possible assignments for this energy level are ν_1, ν_4, and $2\nu_5$. We reject the assignment to ν_4 and $2\nu_5$ because small activity is expected for transitions involving ν_4, ν_5, and ν_6 due to the small Jahn–Teller interaction; we thus assign this line together with lines at 29 828.7 and 30 182.8 cm^{-1} observed in TC-RFWM [correlated with bands B' and C in previous DFWM spectrum

TABLE I. Assignments and vibrational wave numbers (in cm^{-1}) of observed TC-RFWM transitions $\tilde{A}\,^2A_1 \leftarrow \tilde{X}\,^2E_{3/2}$ of CH_3S. Relative to the rotational line at 26 523.2 cm^{-1} in the origin band; line *b* in Fig. 1 was probed. Uncertainties in measurements are listed in parentheses and predicted wave numbers are listed in brackets.

v	3^v	$2^1 3^v$	$1^1 3^v$	$1^1 2^1 3^v$	$2^1 3^1 4^v$
0	0[a]	1095.9[a]	2939.0 (0.2)	3966.2 (0.2)	
1	401.1[a]	1489.9[a]	3305.5 (0.2)	4276.3 [b](0.4) [4322.1]	4358.5[c]
2	794.7[a]	1874.5[c]	3659.6 (0.3)		4667.5[c]
3	1180.6 (0.2)	2252.5 (0.2)			4970.8[c]
4	1558.0 (0.2)	2619.3 (0.2)			
5	1925.6 (0.2)	2973.7[b] (0.3) [2980.3]			
6	2287.2 (0.4)	3324.7[b] (1.3) [3332.3]			
7	2643.9[b](0.4) [2639.5]	3669.0[b,c] [3676.0]			
8	2987.3[b,c] [2983.9]				
$\omega'_{3(0)}$	409.9±0.4	410.2±0.6	410±1	410±0	
x'_{33}	4.10±0.06	4.14±0.07	4.1±0.1	4.15±0.09	
$\omega'_{1(0)}$			2940±1	2940±2	
$\omega'_{2(0)}$		1096.7±0.8		1097±2	
x'_{23}		8.5±0.3		8.6±0.4	
x'_{13}			37.5±0.7	37.5±0.7	
x'_{12}				70±1	

[a]Observed in LIF (Ref. 29).
[b]These lines were excluded from the fitting; see text.
[c]Observed only in DFWM (Ref. 29).

(Ref. 29)] to the $1^1 3^v$ progression with $v=0-2$. Fitting these peak positions by least squares to Eq. (2) with $i=1$, $x'_{11}=0$, and $v'_1=1$ yields $\omega'_{3(0)}=410\pm1$ cm^{-1}, $x'_{33}=4.1\pm0.1$ cm^{-1}, $\omega'_1=2940\pm1$ cm^{-1}, and $x'_{13}=37.5\pm0.7$ cm^{-1}, as listed in Table I. The derived frequency is consistent with *ab initio* predictions, as discussed in detail below, thus confirming our original assignment.

Two additional lines at 30 489.4 and 30 799.5 cm^{-1} above the $1^1 3^2$ line at 30 182.8 cm^{-1} were observed in the TC-RFWM spectra, which correlate with bands *D* and *E* in previous DFWM spectrum.[29] Although these seemed at first to be higher members of the $1^1 3^v$ progression, we ultimately rejected this assignment because: first, the intervals do not follow the pattern observed for the low-lying members of this progression, and second, we found that the first of these bands is *narrower* than the $1^1 3^2$ band, which is unexpected if this band is $1^1 3^3$. Thus, it is clear that these two bands belong to a new progression. As the line at 30 489.4 cm^{-1} corresponds to a vibrational wave number of 3966.2 cm^{-1}, possible assignments for this vibrational level are $\nu_1+\nu_2$, $\nu_4+3\nu_3$, $\nu_2+2\nu_5$, and $\nu_4+\nu_6$. Except the assignment to $\nu_1+\nu_2$, all others involve at least one nontotally symmetric mode and are expected to be weak. We thus assign these two features to the $1^1 2^1$ and $1^1 2^1 3^1$ bands.

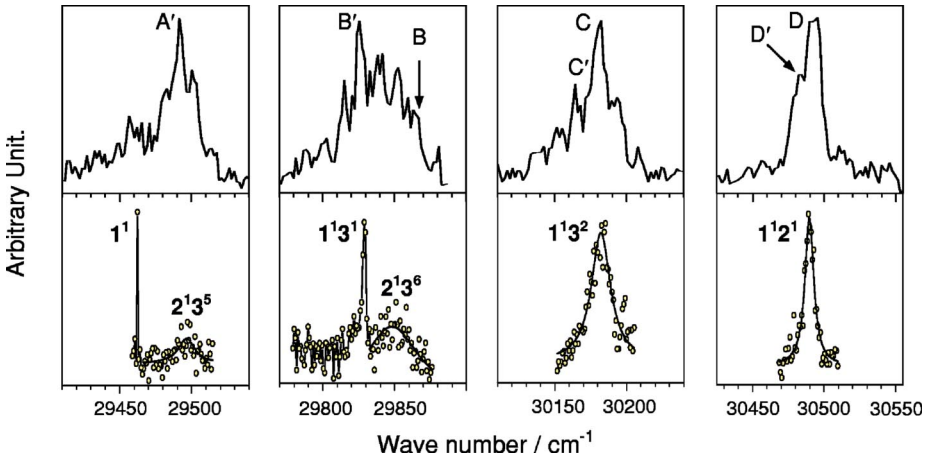

FIG. 3. Comparison of DFWM (upper trace, Ref. 29) and TC-RFWM spectra of the $\tilde{A}$-$\tilde{X}$ system of CH_3S with scan steps 0.01 nm. TC-RFWM bands 1^1 vs $2^1 3^5$ and $1^1 3^1$ vs $2^1 3^6$ demonstrate the pronounced mode specificity observed in this system, with ν_3 a promoting mode for dissociation.

TABLE II. Comparison of vibrational wave numbers (in cm^{-1}) of $\tilde{X}\,^2E_{3/2}$ and $\tilde{A}\,^2A_1$ states of CH_3S and CH_3O.

	CH_3O			CH_3S		
	$\tilde{X}\,^2E_{3/2}$	$\tilde{A}\,^2A_1$		$\tilde{X}\,^2E_{3/2}$	$\tilde{A}\,^2A_1$	
Vibrational mode	Expt.	Expt.	Calc.[a]	Expt.	Expt.	Calc.[b]
$\nu_1(a_1)$	2840	2947.8	3120(2916)	[c]	2940	3186 (2978)
$\nu_2(a_1)$	1412	1289.3	1392(1300)	1313	1097	1240 (1159)
$\nu_3(a_1)$	1047	662.4	759 (709)	727	410	439 (410)
$\nu_4(e)$	2885	3077.8	3281(3066)	[c]		3367 (3147)
$\nu_5(e)$	1465	1403.0	1494(1396)	1496		1488 (1391)
$\nu_6(e)$	1210	929.5	1034 (966)	586	[d]	746 (697)
Ref.	6	6, 42	13	26	29, this work	13

[a]EOM-IP/TZ2P (Ref. 13); values scaled by 0.935 are listed in parentheses.
[b]EOM-IP/6-31G(d,p) (Ref. 13); values scaled by 0.935 are listed in parentheses.
[c]Dispersed fluorescence lists $\nu_1''=2774\ cm^{-1}$ and $\nu_4''=2706\ cm^{-1}$ (Ref. 26).
[d]Proposed to be $635\ cm^{-1}$ in LIF (Ref. 26).

We fit observed lines to an equation involving three vibrational modes (with $x'_{11}=x'_{22}=0$, and $v'_1=v'_2=1$ in this case),

$$\Delta\nu = A + \sum_{i=1}^{3} \omega'_i(v'_i+0.5) - \sum_{i=1}^{3} x'_{i3}(v'_i+0.5)(v'_3+0.5) - x'_{12}(v'_1+0.5)(v'_2+0.5), \quad (3)$$

in which $\Delta\nu$ and A have the same meaning as in Eq. (2), and $\omega'_3=\omega'_{3(0)}+0.5x'_{13}+0.5x'_{23}$. We exclude x'_{11} and x'_{22} from the fitting because information on x'_{11} and x'_{22} from these progressions is lacking. The fitted value $x'_{12}=70\pm1\ cm^{-1}$ indicates a strong interaction between ν_1 and ν_2. Other parameters are similar to those derived from fitting two progressions, as listed in Table I.

Equation (3) was sufficient to fit the wave numbers of all observed lines involving no more than two different vibrational modes. It fails to predict as accurately wave numbers of the $1^12^13^1$ line that involves all three totally symmetric vibrational modes. This line was excluded from the final fit, but is still listed in Table I, along with the corresponding wave number predicted with Eq. (3). The fitting of this line requires the introduction of additional interaction parameters, but such a fitting is unfeasible with only one additional line available for the progression $1^12^13^v$. A similar situation was also observed in the $\tilde{A}$-$\tilde{X}$ system of CF_3S.[41]

Lines at 30 881.7, 31 190.7, and 31 494.0 cm^{-1}, observed in our previous DFWM spectrum, were tentatively assigned as either the $2^13^v4^1$ or $1^12^13^v$ $(v=1-3)$.[29] Now that the latter has been assigned, the only possible assignment for these lines is $2^13^v4^1$. However, wave numbers of these lines cannot be fitted satisfactorily with Eq. (3), as in the case of $1^12^13^v$ discussed above.

It is reasonable to ask why the 1^13^v progression seems to terminate abruptly at $v=3$, when for the 2^13^v and 3^v progressions the Franck–Condon maximum is near $v=3$. As is explained below, the expected line width of 1^13^3 based on the trend observed for the 1^13^v progression exceeds $100\ cm^{-1}$. Thus, a truncation of the 1^13^v progression at $v=2$ is likely due to a broadening of this feature beyond our detection limits.

Table II summarizes observed vibrational wave numbers $\omega'_{i(0)}$ of states $\tilde{A}\,^2A_1$ and $\tilde{X}\,^2E$ of CH_3S and CH_3O;[6,42] the raw and scaled results of theoretical calculations[13] on the $\tilde{A}\,^2A_1$ state are listed for comparison. Experimental vibrational wave numbers of $\tilde{A}\,^2A_1$ states of CH_3S and CH_3O agree well with theoretical calculations when predicted values are scaled by a factor of 0.935; this scaling factor was derived by comparison of predicted values with experiments of CH_3O. Our observation of $\omega'_{1(0)}=2940\ cm^{-1}$ $(\omega'_1=2994\ cm^{-1})$ for CH_3S is slightly greater than the scaled theoretical value of $2978\ cm^{-1}$ and the observation of $\omega'_{2(0)}=1097\ cm^{-1}$ $(\omega'_2=1136\ cm^{-1})$ is slightly smaller than the scaled theoretical value $1160\ cm^{-1}$ both are within expected error limits.

C. Predissociation of the $\tilde{A}\,^2A_1$

In general, the total line-shape function of the TC-RFWM signal involves integration over the velocity distribution and is difficult to express in a simple analytic form, being dependent on relaxation processes and lifetimes of the states involved.[43] However, in the limiting case in which homogeneous broadening dominates, the line-shape function can be approximated with a simple Lorentzian squared function, as shown previously.[39,44] To account for the laser line width, we fit the observed line profile to the square of a Voigt function using a nonlinear least-squares routine. The Gaussian component was fixed to reproduce the laser-limited line width $(\sim0.2\ cm^{-1})$ observed in the four lines $(3^3,\ 3^4,\ 2^13^3,$ and $1^1)$ for which no lifetime broadening was observed.

The predissociation lifetime τ is related to the Lorentzian line width by

$$\tau = 1/2\pi c\Gamma \quad (4)$$

in which c is the speed of light in cm s^{-1} and Γ is the FWHM in cm^{-1}. Lifetimes of predissociative levels thus estimated from observed line widths are listed in Table III; each listed value is the mean of at least five independent measurements and the errors represent one standard deviation. The data are plotted in Fig. 4 for comparison. We did not make a concerted effort to explore the power dependence of the TC-

TABLE III. Vibrational wave numbers, assignments, and lifetimes for the $\tilde{A}\,^2A_1$ state of the CH_3S radical.

Wave numbers (cm^{-1})	Assignment	Lifetimes: Chiang and Lee[a] (ns)	Lifetimes: Pushkarsky *et al.*[b] (ns)	Lifetimes: This work (ps)	Lifetimes: Bise *et al.*[c] (ps)
26 526.7[d]	0^0	1130 (70)	1090 (55)		
26 927.6[d]	3^1	860 (30)	870 (40)		
27 321.4[d]	3^2	250 (20)	300 (30)		
27 622.6[d]	2^1	480 (30)	460 (30)		
27 707.2[e]	3^3	72 (30)	$\leqslant$35	[f]	
28 015.6[d]	2^13^1	85 (15)	60 (20)		
28 084.7[e]	3^4		$0.010<\tau<10$	[f]	25
28 398.9[d]	2^13^2		$0.010<\tau<10$		
28 452.6[e]	3^5		0.0015 (3)	1.55(14)	10
28 779.1[e]	2^13^3		$0.010<\tau<10$	[f]	25
28 812.6[e]	3^6		0.0004 (1)	0.48(10)	4
29 145.9[e]	2^13^4		0.0010 (2)	1.09(14)	8
29 170.0[e]	3^7		0.0005 (1)	0.53(13)	2
29 462.2	1^1			[f]	
29 500.4	2^13^5		0.0004 (1)	0.35 (6)	
29 828.7	1^13^1			1.5 (2)	
29 851.4	2^13^6			0.09 (5)	
30 182.8	1^13^2			0.28 (3)	
30 489.4	1^12^1			0.46 (3)	
30 799.5	$1^12^13^1$			0.35(10)	

[a]Reference 26.
[b]Reference 28.
[c]Reference 27.
[d]Observed only in LIF or DFWM (Ref. 29).
[e]Listed wave numbers are from TC-RFWM spectra with line *a* in Fig. 1 probed, whereas their widths were averages of those measured from TC-RFWM spectra with both lines *a* and *b* in Fig. 1 probed. Lines above 29 170 cm^{-1} are from spectra with line *b* probed.
[f]Laser-limited linewidth.

RFWM signal; however, based on our qualitative observations of the signal to laser power, it seems clear that we were not in the power saturation regime. The linewidths observed for the strongest transition (3^3) are consistent with expected laser linewidth; it would be more difficult to saturate highly dissociative transitions. Our results for the 3^v and 2^13^v progressions are consistent with measurements of Pushkarsky and Miller using fluorescence depletion,[28] which are listed in Table III for comparison. This is important confirmation of the validity of our data reduction procedures. We also include in Table III the results of Bise *et al.*,[27] who used an indirect method to estimate the lifetimes. Their reported values are overestimated in comparison with those obtained in our measurements and those of Pushkarsky and Miller.

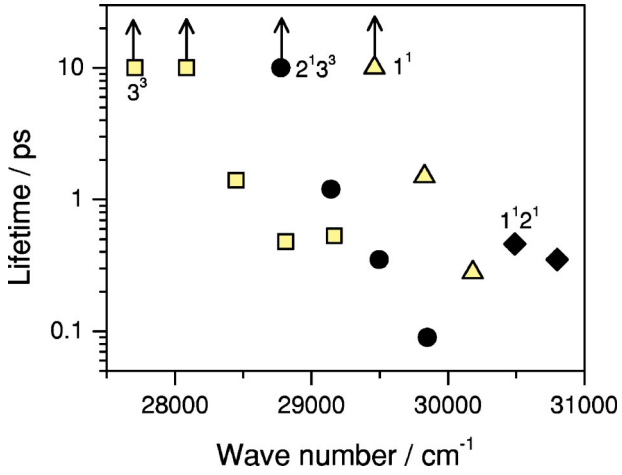

FIG. 4. Dependence of lifetimes in the $\tilde{A}\leftarrow\tilde{X}$ system on vibrational mode and energy in TC-RFWM experiments. Progressions 3^v (□, $v=3$–7), 2^13^v (●, $v=3$–6), 1^13^v (△, $v=0$–2), and $1^12^13^v$ (◆, $v=0$ and 1) are marked with different symbols. The arrows indicate bands for which no lifetime broadening was observed, indicating that the lifetime exceeds ~10 ps.

The lifetimes of the 1^13^v and $1^12^13^v$ progressions were determined here for the first time. Previous work has shown that levels above 27 321.4 cm^{-1} (3^2) are highly predissociative, but the 1^1 line at 29 462.2 cm^{-1} showed no evidence of lifetime broadening. However, the addition of one quanta of ν_3 leads to a tenfold decrease in lifetime, illustrating the mode specificity in the dissociation previously revealed for the 3^v and 2^13^v progressions by Pushkarsky *et al.*[28] Figure 3 shows other examples of this mode specificity, and the trend observed in each progression in Fig. 4 clearly demonstrates that ν_3 is a promoting mode for dissociation. Comparing the levels 2^1 ($\tau\sim$480 ns), 1^1 (10 ps$<\tau<$10 ns), and 1^13^1 ($\tau\sim$0.46 ps), we discern that the rate of predissociation is also a function of energy. We look forward to theoretical studies on the predissociation rates in this system.

IV. CONCLUSION

We demonstrate the advantages of two-color resonant four-wave mixing in investigating highly predissociated lev-

els of CH_3S in its $\tilde{A}\,^2A_1$. We confirmed vibrational assignments of new progressions $1^1 3^v$ and $1^1 2^1 3^v$ involving the symmetric CH_3 stretching mode (ν_1) and measured quantitatively their lifetimes. The vibrational wave number is $\nu_1 = 2940\ \mathrm{cm}^{-1}$, consistent with theoretical calculations. The spectra show pronounced mode specificity with ν_3 a clear promoting mode for dissociation.

ACKNOWLEDGMENTS

The authors thank the National Science Council of Taiwan (Grant No. NSC93-2119-M-009-002) and MOE Program for Promoting Academic Excellence of Universities (Grant No. 89-FA04-AA) for support. S.A.R. thanks the National Science Council of Taiwan for a visiting professorship at the National Tsing Hua University and acknowledges the Petroleum Research Fund, administered by the American Chemical Society.

[1] R. J. Charlson, J. E. Lovelock, M. O. Andreae, and S. G. Warren, Nature (London) **326**, 655 (1987).
[2] T. S. Bates, B. K. Lamb, A. Guenther, J. Dignon, and R. E. Stoiber, J. Atmos. Chem. **14**, 315 (1992).
[3] A. R. Ravishankara, Y. Rudich, R. Talukdar, and S. B. Barone, Philos. Trans. R. Soc. London, Ser. B **352**, 171 (1997).
[4] G. S. Tyndall and A. R. Ravishankara, Int. J. Chem. Kinet. **23**, 483 (1991).
[5] J. M. C. Plane, in *Biogenic Sulfur and in the Environment*, edited by E. S. Saltzman and W. J. Cooper (American Chemical Society, Washington, D.C., 1989).
[6] D. E. Powers, M. B. Pushkarsky, and T. A. Miller, J. Chem. Phys. **106**, 6878 (1997).
[7] B. E. Applegate, M. B. Pushkarksky, and T. A. Miller, J. Phys. Chem. A **103**, 1538 (1999).
[8] G. D. Bent, J. Chem. Phys. **92**, 1547 (1990).
[9] G. D. Bent, J. Chem. Phys. **89**, 7298 (1988).
[10] R. Fournier and A. E. Depristo, J. Chem. Phys. **96**, 1183 (1992).
[11] C.-W. Hsu, C.-L. Liao, Z.-X. Ma, P. J. H. Tjossem, and C. Y. Ng, J. Chem. Phys. **97**, 6283 (1992).
[12] A. C. Curtiss, R. H. Nobes, J. A. Pople, and L. Radom, J. Chem. Phys. **97**, 6766 (1992).
[13] Q. Cui and K. Morokuma, Chem. Phys. Lett. **263**, 54 (1996).
[14] R. D. El Bouzaidi, A. El Hammadi, A. Boutalib, and M. El Mouhtadi, J. Mol. Struct.: THEOCHEM **497**, 197 (2000).
[15] A. B. Callear, J. Connor, and D. R. Dickson, Nature (London) **221**, 1238 (1969).
[16] A. B. Callear and D. R. Dickson, Trans. Faraday Soc. **66**, 1987 (1970).
[17] K. Ohbayashi, H. Akimoto, and I. Tanaka, Chem. Phys. Lett. **52**, 47 (1977).
[18] P. C. Engelking, G. B. Ellison, and W. C. Lineberger, J. Chem. Phys. **69**, 1826 (1978).
[19] B. K. Janousek and J. I. Brauman, J. Chem. Phys. **72**, 694 (1980).
[20] S. Moran and G. B. Ellison, J. Phys. Chem. **92**, 1794 (1988).
[21] Y. Endo, S. Saito, and E. Hirota, J. Chem. Phys. **85**, 1770 (1986).
[22] M. Suzuki, G. Inoue, and H. Akimoto, J. Chem. Phys. **81**, 5405 (1984).
[23] G. Black and L. E. Jusinski, J. Chem. Soc., Faraday Trans. 2 **82**, 2143 (1986).
[24] G. Black and L. E. Jusinski, J. Chem. Phys. **85**, 5379 (1986).
[25] Y.-C. Hsu, X. Liu, and T. A. Miller, J. Chem. Phys. **90**, 6852 (1989).
[26] S.-Y. Chiang and Y.-P. Lee, J. Chem. Phys. **95**, 66 (1991).
[27] R. T. Bise, H. Choi, H. B. Pedersen, D. H. Mordaunt, and D. M. Neumark, J. Chem. Phys. **110**, 805 (1999).
[28] M. B. Pushkarsky, B. E. Applegate, and T. A. Miller, J. Chem. Phys. **113**, 9649 (2000).
[29] C.-P. Liu, Y. Matsuda, and Y.-P. Lee, J. Chem. Phys. **119**, 12335 (2003).
[30] Y.-Y. Lee, S.-Y. Chiang, and Y.-P. Lee, J. Chem. Phys. **93**, 4487 (1990).
[31] R. L. Farrow, D. J. Rakestraw, and T. Dreier, J. Opt. Soc. Am. B **9**, 1770 (1992).
[32] W.-C. Hung, M.-L. Huang, Y.-C. Lee, and Y.-P. Lee, J. Chem. Phys. **103**, 9941 (1995).
[33] A. Kumar, C.-C. Hsiao, W.-C. Hung, and Y.-P. Lee, J. Chem. Phys. **109**, 3824 (1998).
[34] X. Li, A. Kumar, C.-C. Hsiao, and Y.-P. Lee, J. Phys. Chem. A **103**, 6162 (1999).
[35] X. Li and Y.-P. Lee, J. Chem. Phys. **111**, 4942 (1999).
[36] A. Kumar, C.-C. Hsiao, W.-C. Hung, and Y.-P. Lee, Chem. Phys. Lett. **269**, 22 (1997).
[37] Y. Tang, J. P. Schmidt, and S. A. Reid, J. Chem. Phys. **110**, 5734 (1999).
[38] A. Kumar, C.-C Hsiao, Y.-Y. Lee, and Y.-P. Lee, Chem. Phys. Lett. **297**, 300 (1998).
[39] S. Williams, J. D. Tobiason, J. R. Dunlop, and E. A. Rohlfing, J. Chem. Phys. **103**, 9941 (1995).
[40] SpecView: Simulation and Fitting of Rotational Structure of Electronic and Vibronic Bands. V. Stakhursky and T. A. Miller, 56th Molecular Spectroscopy Symposium. http://molspect.mps.ohio-state.edu/goes/specview.html
[41] D. E. Powers, M. B. Pushkarsky, M.-C. Yang, and T. A. Miller, J. Phys. Chem. A **101**, 9846 (1997).
[42] S. C. Foster, P. Misra, T.-Y. D. Lin, C. P. Damo, C. C. Carter, and T. A. Miller, J. Phys. Chem. **92**, 5914 (1988).
[43] S. Williams, E. A. Rohlfing, L. A. Rahn, and R. N. Zare, J. Chem. Phys. **106**, 3090 (1997).
[44] S. Williams, R. N. Zare, and L. A. Rahn, J. Chem. Phys. **101**, 1072 (1994).